Hindawi
Mobile Information Systems
Volume 2022, Article ID 2078191, 13 pages
https://doi.org/10.1155/2022/2078191

Research Article

Changes of Remote Sensing Data in Urban Buildings Based on Neural Network Algorithm

Li Xue, Fanmin Meng, and Chaoran Li

School of Management, Shenyang Jianzhu University, Shenyang 110168, Liaoning, China

Correspondence should be addressed to Li Xue; xueli1965@sjzu.edu.cn

Received 9 May 2022; Revised 23 August 2022; Accepted 3 September 2022; Published 22 September 2022

Academic Editor: Imran Shafique Ansari

Copyright © 2022 Li Xue et al. This is an open access article distributed under the Creative Commons Attribution License, which permits unrestricted use, distribution, and reproduction in any medium, provided the original work is properly cited.

Remote sensing data refer to remote sensing data sets with typical big data characteristics obtained by various remote sensing technologies. Based on this understanding, massive remote sensing datasets are the main method, and auxiliary data from other sources are integrated. The DN value (digital number) is the brightness value of the remote sensing image pixel and the gray value of the recorded ground objects. Unitless is an integer value. The value is related to the sensor's radiation resolution, ground object emissivity, atmospheric transmittance, and scattering rate. This study aims to study the neural network algorithm for remote sensing data changes in urban buildings. This study deliberately goes to Tianjin Binhai New Area, taking this as an example to analyze and study the change of construction land. It uses satellite remote sensing data as a basis to analyze the trend of its building land. This study proposes which factors lead to the decline of urban construction land in Tianjin Binhai New Area. Finally, through experimental research and analysis, it is found that from 1996 to 2016, the registered population of Tianjin Binhai New Area has increased a lot, accounting for 26.49% of the total population. The number of urban employees increased by 956,500. This is also the leading factor in the direction of the city for the building.

1. Introduction

A city is a complex "natural economy" ecosystem established by human beings in the process of adapting and transforming the natural environment. It is an irreversible change in the way of utilization, which has a huge impact on human activities. Since the reform and opening up, the starting point of China's urbanization development is relatively low, but its development speed is indeed very fast. Urbanization refers to the process, in which construction land occupies a large amount of agriculture, forestry, animal husbandry, and water bodies. It greatly changes the actual land cover probability in the area. The changes of urban land use profoundly reflect the changing laws of urbanization process and spatial structure. The theme of satellite remote sensing technology is the development trend of cities over the years. The researcher extracts building information, mainly for the monitoring of changes in urban construction, urban infrastructure planning, 3D urban reconstruction, digital cities, urban land use and management, and real-time updates of urban rail and traffic maps. How to achieve high-efficiency, high-precision, and automatic extraction of buildings in urban areas is the difficulty and focus of research in remote sensing image processing.

Urban spatial expansion is the most intuitive physical manifestation of urbanization, and it is also the most important feature of land cover change. The expansion of urban space and the evolution of external form are the inevitable trends of urban development. Different characteristics of urban development are presented in different stages and directions. However, the urban landscape is relatively unique, with obvious fragmentation and serious damage to natural ecological functions. This leads to serious ecological problems such as urban heat islands, reduction of agricultural land, wetland degradation, and air and water pollution and also leads to a decline in the quality of human settlements and the healthy development of cities. Most remote sensing images are not ortho-satellite images. Therefore, in the remote sensing images, the target objects are often inclined or blocked by the shadows of other objects such as

trees and high-rise buildings. Moreover, with the gradual increase of the observation scale of satellites, there will be many phenomena of the same spectrum of different objects and the phenomenon of different spectrums of the same objects. Under the current environment of strengthening ecological environment management and optimizing the development pattern of King's space, it is of great significance to the urban planning of Suqian to study the changes of King's land cover and urban expansion in Suqian as a prefecture-level emerging small city. It is necessary to optimize the land cover and industrial layout of the king, recognizing the future ecological environment construction.

This study mainly studies the trend of urban construction in Tianjin Binhai New Area and analyzes its causes. It introduces neural network algorithms to ensure thorough data analysis and more accurate conclusions. The innovation of this study lies in the continuous improvement of the neural network algorithm as well as on-the-spot investigation and research. This is to ensure the accuracy of the data. It has also been innovating and refining its own team to make it more efficient.

The second part of the article mainly introduces the research and development of urbanization construction at home and abroad and the application of its remote sensing network data. The third part mainly introduces the neural network algorithm and its improvement technology. Finally, the fourth part uses remote sensing network technology in the experimental part. The urbanization construction land of Tianjin Binhai New Area is deeply researched and analyzed and then discussed in Section 5. Finally, the experimental results in Section 6 show that the main factors affecting the change of construction land are population growth, economic development, and construction of transportation facilities.

2. Related Work

The rapid development of society has driven rapid economic growth, population agglomeration, and expansion of construction land. This also leads to resource and environmental problems to a certain extent, such as farmland loss, soil pollution, and erosion. The use of remote sensing technology can quickly and effectively obtain construction land information for extraction. It can provide a scientific and timely data basis for construction and decision-making departments. Urban architecture is an important part of current research, and more and more researchers pay special attention to it. Among them, Liu studied the remote sensing image data and nighttime lighting data of this area [1]. Remote sensing techniques are increasingly used to rapidly detect and visualize changes caused by catastrophic events. Sofina and Ehlers proposed a feature-based semiautomatic method to identify building conditions, especially affected areas using geographic information system (GIS) and remote sensing information [2]. The growth of world population has triggered the increase of artificial surfaces such as buildings and roads in urban areas. Atak and Tonyalolu aimed to analyze the impact of changes in LULC, NDVI, and LST in Ayton, Turkey between 1990 and 2017 [3]. Over the past few decades, many countries and regions have increasingly considered land-use change, sprawl, and its impact on natural lands (gardens, agriculture, and arable land). However, the analytical knowledge of land-use change and urban sprawl due to natural land loss remains unclear. Therefore, Dadashpoor and Salarian aimed to use data including remotely sensed satellite images from 1986, 1996, 2006, and 2015 (LandsatTM) to analyze and predict the trend of urban construction land use change and sprawl from 1986 to 2040 [4]. However, the methods used for urban construction are not very efficient and lack innovation.

With the development of remote sensing (RS) and deep learning (DL) technologies, various forms of data for detecting land use changes are available. The goal of Ji and Luo is to promote the coordinated development of land use [5]. Remote sensing data can be used to improve understanding of environmental changes over longer periods of time. Here, Frankl et al. used aerial photographs and satellite imagery to explore trends and patterns of woody vegetation cover in the Lake Tana Basin [6]. In the following work, Alshehhi et al. proposed a single-patch-based convolutional neural network (CNN) architecture for extracting roads and buildings from high-resolution remote sensing data [7]. They all made good use of remote sensing technology, made a certain analysis of urban land construction, and obtained corresponding results, but the analysis was not comprehensive enough, lacked innovation, and was not authoritative.

3. Neural Network Algorithm

3.1. Classification of Neural Network Algorithms

3.1.1. Single Layer Neural Network. Figure 1 shows a graphical explanation of the perceptron model.

In Figure 1(a), the weight (q_1, q_2, q_3) is added to the perceptron, and the calculation formula of the output unit is as follows:

$$z_1 = x_1 \otimes q_1 + x_2 \otimes q_2 + x_3 \otimes q_3. \tag{1}$$

In Figure 1(b), the weight $(q4q_5, q_6)$ is added to the perceptron, and the calculation formula of the output unit is as follows:

$$z_2 = x_1 \otimes q_4 + x_2 \otimes q_5 + x_3 \otimes q_6. \tag{2}$$

3.1.2. Two-Layer Neural Network. $x^{(1)}\mathrm{x}^{(2)}$ Z is the data transmitted in the network, $\mathrm{q}^{(1)}q^{(2)}$ is the weight in the network, and $\mathrm{y}^{(1)}y^{(2)}$ is the bias term in the network. The two-layer neural network without bias term is calculated as follows [8]:

$$\begin{cases} \mathrm{x}^{(1)} \otimes q^{(1)} = x^2 \\ \mathrm{x}^{(2)} \otimes q^{(2)} = z \end{cases} \begin{cases} \mathrm{x}^{(1)} \otimes q^{(1)} + \mathrm{y}^{(1)} = x^2 \\ \mathrm{x}^{(2)} \otimes q^{(2)} + y^{(2)} = z \end{cases}. \tag{3}$$

3.1.3. Multilayer Neural Network. Visible units constitute explicit layers for input training data. Hidden units form hidden layers for resource detection. When the value of all

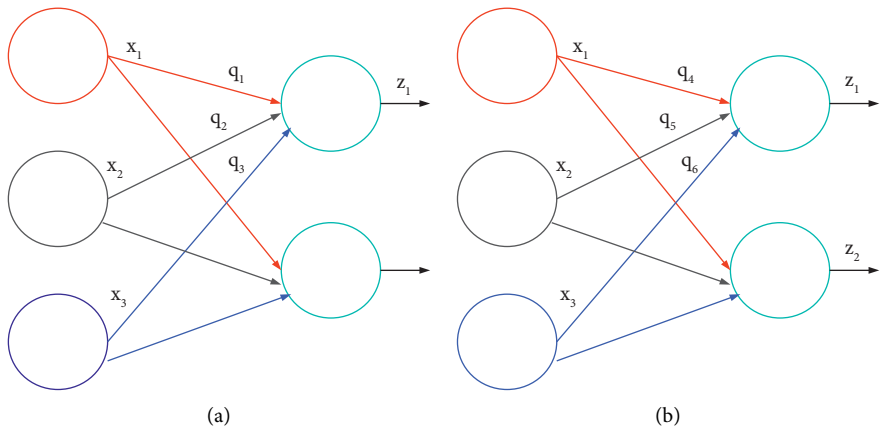

Figure 1: Perception model diagram.

explicit elements is given, the value of each implicit element is irrelevant, for example,

$$p(g|d) = \prod_{i=1}^{m} p(g_i|d). \tag{4}$$

When the values of all hidden layers are given, the values of all explicit elements are also not correlated, as shown in the following formula:

$$p(\mathrm{d}|g) = \prod_{j=1}^{n} p(d_j|g). \tag{5}$$

Among them, d is the visible layer and $g^1 g^2 g^3$ is the hidden layer. This layer is a hidden layer. The goal of its algorithm is to train hidden layer units and allow them to extract correlations between higher-order data belonging to visible layer D. The output calculation of the visual layer is shown in the following formula:

$$\begin{aligned} &\mathrm{p}\left(d, g^1, g^2, \ldots, \ldots g^1\right) \\ &\quad = p\left(d \mid g^1\right) p\left(g^1 \mid g^2\right) \ldots p\left(g^{l-2} \mid g^{l-1}\right) p\left(g^{l-1}, g\right). \end{aligned} \tag{6}$$

3.2. Convolutional Neural Networks. It includes convolution computation and is one of the algorithms of deep learning [9]. After the feature map is obtained through the convolution operation, the extracted features are used for classification or segmentation operations. The convolutional neural network structure includes an input layer and a hidden layer. The hidden layer includes three common structures: convolutional layer, pooling layer, and fully connected layer. In some more modern algorithms, there may be complex constructions such as inception modules and residual blocks. In common constructions, convolutional layers and pooling layers are specific to convolutional neural networks. For example, if each of the 100 features is convolved with an image, a $(256 - 32 + 1) \times (256 - 32 + 1) = 50625$-dimensional convolution feature will be obtained. Since there are 100 features, each input will get a $50625 \times 100 = 5062500$-dimensional feature vector [10]. It is unwise for a neural network to learn a classifier with more than five million dimensional features in the input data [11]. Moreover, the phenomenon of overfitting is easy to occur in the process of network training. The so-called overfitting is a phenomenon as follows: a hypothesis can obtain a better fit than other hypotheses on the training data but cannot fit the data well on the data set other than the training data. At this point, we call this assumption overfitting. Its max pooling is shown in Figure 2.

The research on convolutional neural networks can be traced back to the neocognitron model proposed by Japanese scholar Kunihiko Fukushima. In his papers published in 1979 and 1980, Fukushima designed a neural network named "neocognitron" for the visual cortex of a living creature. Neocognitron is a neural network with deep structure, and it is one of the earliest proposed deep learning algorithms. In 2001, scientists observed and studied the energy consumption process of biological brains. In 2003, it was estimated that only 1% to 4% of neurons can be activated by the brain at the same time. This study confirms the sparsity of how neurons are encoded. From the signal point of view, the neuron only responds to a small part of the input. A large number of input signals are ignored by neurons. But doing so, we can improve the learning efficiency and allow the neural network to extract features more accurately and quickly. The sparse connections of convolutional neural networks have a regularization effect. It improves the stability and generalization ability of the network structure and avoids overfitting. At the same time, sparse connections reduce the total amount of weight parameters. This facilitates fast learning of neural networks and reduces memory overhead during computation. After initializing the weight parameters, the traditional sigmoid activation function activates nearly half of the neurons. This violates the way neurons are sparsely encoded. Linear rectification function, also known as modified linear unit, is an activation function commonly used in artificial neural networks. It usually refers to nonlinear functions represented by ramp functions and their variants. Subsequently, the researchers found that the rectified linear unit (ReLu) activation function is much better than the sigmoid activation function [12]. Convolutional neural network has long

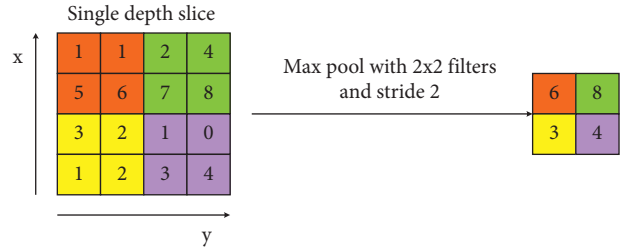

Figure 2: Max pooling.

been one of the core algorithms in the field of image recognition and has a stable performance when the learning data are sufficient. For general large-scale image classification problems, convolutional neural networks can be used to construct hierarchical classifiers. It can also be used in fine-grained recognition to extract discriminative features of images for learning by other classifiers.

The mathematical form of the ReLu activation function is as follows:

$$f(a) = \max(0, a). \tag{7}$$

3.3. Overview of the Study Area. Before the emergence of popular deep learning methods, the research on automatic extraction of buildings and other objects in remote sensing images based on traditional feature extraction methods can achieve high accuracy [13]. But the biggest disadvantage of the traditional method is the single feature. *Generalization Ability*. The functional ability of deep learning methods is actually determined by the method itself, that is, whether there is a necessary connection between the feature and the target [14, 15]. For example, the traditional Hough transform performs feature extraction based on fixed features such as lines, angles, and surfaces. In increasingly prosperous urban areas, there are fewer and fewer regular, simple building appearances. Therefore, more feature detectors and feature extractors are needed to accommodate this change. Obviously, traditional nondepth methods are no longer competent and instead are replaced by deep algorithms with strong feature generalization and extraction capabilities [16]. Based on the idea of deep learning, this study proposes a cascaded fully convolutional neural network structure. It adopts the methods of resource reuse and resource enhancement to realize the automatic and accurate extraction of urban buildings in satellite images. Its process model diagram is shown in Figure 3:

This area is near the Tanggu Railway Station in Binhai New Area, Tianjin. It includes residential areas, hospitals, schools, roads, railways, vegetation and water bodies, and other types of features. The buildings are irregularly distributed and of various types. It exhibits different spectral and spatial characteristics. The background environment is complex and contains many disturbing objects, which is more representative as a research area [17, 18].

This study takes Tianjin Binhai New Area as an example to analyze the change of construction land. Tianjin is one of the municipalities directly under the Central Government in China, located in the northeastern region of China, between 38°34′–40°15′N, 116°43′–118°04′E. It is the economic center of the Bohai Rim region. Binhai New Area has a long history, rich natural resources, and advantageous geographical conditions [19, 20]. It is one of 16 districts. Binhai New Area is located in the northern plains of China, east of Tianjin, downstream of the Haihe River, and adjacent to the Bohai Sea. Binhai New Area has a large port, Tianjin Port, which is China's international transportation and logistics center. Tianjin Binhai New Area is mainly composed of Dagang District, Hangu District, Tanggu District, and Tianjin economic and technological development zone. It is an important area for China's economic development. The development potential is huge, the natural resources are abundant, and the ecological environment is good. Tianjin Binhai New Area has 18 towns under its jurisdiction, which can be divided into nine functional areas, including the central business district, the airport economic zone, and the Nangang industrial zone. Since its establishment, Tianjin Binhai New Area has developed rapidly due to its advantages in geographical location, natural resources, economic development, and other aspects. The foreign population is large and the mobility is high. As of 2016, it includes a resident population of about 2.9942 million and a registered population of about 1.2818 million. The construction land changes rapidly and has a certain application value as a research area.

3.4. Data Sources. When comparing construction land extraction methods, a SPOT6 image acquired in April 2014 and a Landsat8 image acquired in the same month of the same year were selected. Since the SPOT series satellites were put into use, they have provided a large number of rich and reliable global remote sensing satellite data sources for various application fields. SPOT6 data have high spatial resolution and strong data acquisition capability. The SPOT6 and SPOT7 double-star constellations enable one-day revisiting of any location on Earth. The SPOT6 image has a width of 60×60 km, including one panchromatic band and four multispectral bands. The specific satellite parameters are listed in Table 1. The multispectral data and panchromatic data of SPOT6 have their own RPM (RigorousPhysicalModel) model parameter file (Dim.XML metadata file) and RFM (RationalFunctionModel) model parameter file (RPC.XML file), which are used to assist SPOT6 orthorectification.

Taking Tianjin Binhai New Area as the study area, the Landsat series of satellites are remote sensing satellite systems used to develop and construct the Earth resources and environment. Landsat5 was successfully launched in 1984 and Landsat8 was launched successfully in 2013 with a temporal resolution of 16 days. The data sources used to analyze the changes of building land are Landsat5 remote sensing images in 1996, 2001, 2006, and 2011, and Landsat8 remote sensing images in 2016. The specific satellite parameters are listed in Tables 2 and 3. In addition to infrared sensors (infrared sensors), it can also carry two remote sensing infrared satellites. The Landsat5 and Landsat8 remote sensing image data used in this study are from the United States Geological Survey website [21, 22]. The United States Geological Survey (USGS) is a scientific research

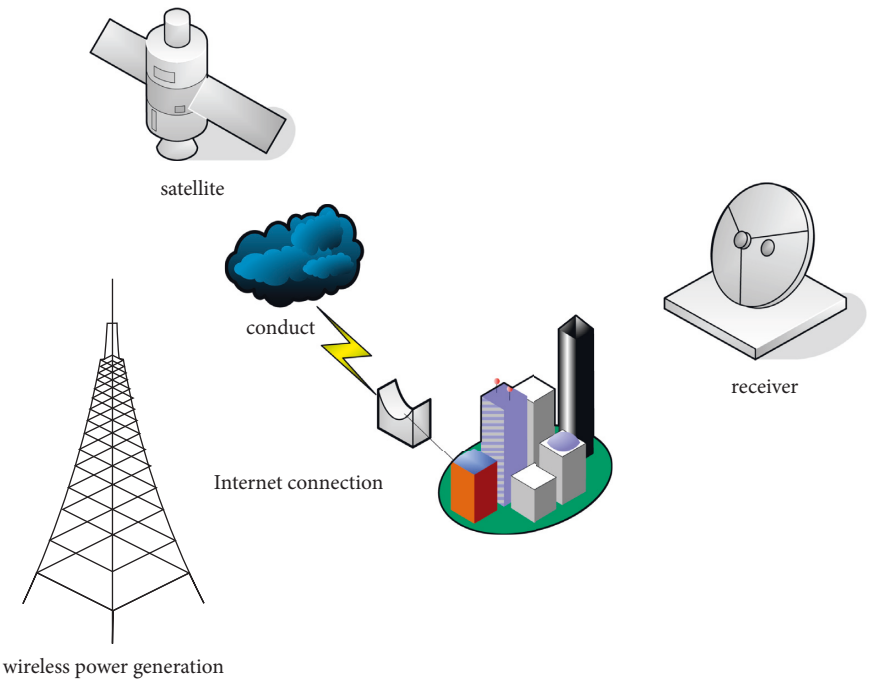

Figure 3: Model diagram of automatically extracted buildings from remote sensing images.

Table 1: Landsat satellite parameters.

Band	Spectral range	Spatial resolution	Height	Revisit period (days)
*B*1	0.433–0.453	30	185 × 185	16
*B*2	0.450–0.515			
*B*3	0.525–0.600			
*B*4	0.630–0.680			
*B*5	0.845–0.885	115		
*B*6	1.560–1.660			
*B*7	2.100–2.300			
*B*8	0.500–0.680			
*B*9	1.360–1.390	30		
*B*10	10.600–12.500	100		

Table 2: Convolutional layer parameter setting table.

Network layer ID	Size
Conv1-1	3 × 3 × 64
Conv1-2	3 × 3 × 64
Maxpooling	2 × 2
Conv2-1	3 × 3 × 128
Conv2-2	3 × 3 × 128
Maxpooling	2 × 2
Conv3-1	3 × 3 × 256
Conv3-2	3 × 3 × 256
Conv3-3	3 × 3 × 256
Maxpooling	2 × 2

institution affiliated to the United States Department of the Interior. It is responsible for scientific research, monitoring, collection, and analysis of natural disasters, geology, mineral resources, geography and environment, and wildlife information [23, 24]. It conducts nationwide long-term monitoring and assessment of natural resources. It provides broad, high-quality, and timely scientific information to policymakers and the public [25].

Table 3: Contribution rate of construction land expansion in Dagang District, Hangu District, Tanggu District, 1996–2016 (unit: %).

Year range	Tanggu District	Hangu District	Dagang District
1996–2001	48.90	36.60	14.49
2001–2006	69.71	14.49	15.80
2006–2011	91.26	0.82	7.92
2011–2016	59.64	16.56	23.80
1996–2016	69.60	13.06	17.34

4. Experiment of Remote Sensing Data in Urban Building Changes

4.1. Improvement of Convolutional Neural Network Algorithm. The original remote sensing image is defined as *v*, as shown in the following formula:

$$V = \left\{V^{(1)} \cap V^{(2)} \cap \ldots V^{j} \ldots \cap V^{(m-1)} \cap V^{(m)}\right\}. \quad (8)$$

Among them, $V^{(j)}$ is a single multiband high-resolution satellite remote sensing image.

The multichannel pixel-level label image is defined as viewing *k*, as shown in the following formula:

$$K = \left\{K^{(1)} \cap K^{(2)} \cap \ldots K^{j} \ldots \cap K^{(m-1)} \cap K^{(m)}\right\}. \quad (9)$$

Among them, $K^{(j)}$ is a single-label image. The label image is also known as the ground truth. It is a single-label image, also known as the ground truth. All received remote

sensing images are treated as a series of w combinations of image patches. W is represented as follows:

$$W = \left\{\left(\vec{V}_j, \vec{K}_j\right), j = 1, 2, 3, \ldots m\right\}. \tag{10}$$

Among them, $\vec{V}_j$ is an image block of a remote sensing image in the original remote sensing image $V^{(j)}$. $\vec{K}_j$ is an image block of a certain tag image in the original tag image $K^{(j)}$.

Now, we predict the label image patch $\vec{K}_j$ from the remote sensing image patch $\vec{V}_j$. The image block prediction result is defined as $P(\vec{V}_j \mid \vec{K}_j)$, and the overall prediction result $P(\vec{V}_j \mid \vec{K}_j)$ is as follows:

$$P(\vec{K} \mid \vec{V}) = \prod^{mn} P\left(\vec{K}_j \mid \vec{V}_j\right), \tag{11}$$

$F_j(\vec{K})$ is defined as the value that the prediction result of the jth image patch is a building. It is calculated as follows:

$$\begin{aligned} F_j(\vec{K}) &= \text{Sigmoid}\left(m_j(\vec{k})\right), \\ \text{Sigmin d}(a) &= \frac{1}{(1 + \exp(-a))}. \end{aligned} \tag{12}$$

Among them, $m_j(\vec{k})$ is the image block of the jth remote sensing image.

The expression for convolution in calculus is as follows:

$$e(d) = \int a(d - x)\beta(x)tx. \tag{13}$$

If it is in discrete form, the formula is as follows:

$$e(d) = \sum_x a(d - x)\beta(x). \tag{14}$$

If it is a two-dimensional convolution, it can be expressed as follows:

$$e(j, i) = \sum_n \sum_m a(j - n, i - m)\beta(n, m). \tag{15}$$

In convolutional neural networks, although the basic unit is convolution, it is a little different from the strict mathematical definition. The convolution calculation in the neural network is as follows:

$$e(j, i) = \sum_n \sum_m a(j + n, i + m)\beta(n, m) + s. \tag{16}$$

The volume multiplies the elements of the different local arrays of the output image and the convolution kernel array and then adds them together, and the output matrix is a 2×3 matrix. Convolutional neural networks need to rotate the convolution kernel by 180°.

The parameter settings of the convolutional layer in this study are listed in Table 2.

The loss function is the objective function of neural network optimization, as follows:

$$\text{Cost} = \frac{1}{2n}\sum_a [b(a) - x(a)]^2. \tag{17}$$

Among them, b (a) is the expected output and $x(a)$ is the actual output. For a neuron, the relationship between the input value x and the corresponding output a is as follows:

$$\begin{cases} w = \varphi a + y \\ x = \varepsilon(w) \end{cases}. \tag{18}$$

Then the corresponding partial derivatives can be obtained, as follows [17]:

$$\begin{cases} \dfrac{\eta Cost}{\eta \beta} = (\varphi(w) - b)\beta'(w)a \\ \dfrac{\eta Cost}{\eta y} = (\varphi(w) - b)\beta'(w) \end{cases}. \tag{19}$$

4.2. Data Processing. For improving the classification accuracy of land use types, the role of image fusion is more important than atmospheric correction. Therefore, image fusion is a key step in data preprocessing. There are many methods of image fusion. In this study, the transform fusion method is used to fuse multispectral images and panchromatic images. Through the statistical analysis, the GS fusion method performs orthogonal transformation on multidimensional images to eliminate information redundancy and improve the problem of inconsistent spectral response or excessive concentration of information in some image bands. The PC transformation method usually has two cases: one is to replace the first principal component PC1 of the multiband image with a high-resolution image. The second is to perform the principal component transformation on all the bands of the multiband image. Compared with PC transformation, GS transformation can better preserve the spectral information of the image. In this study, the multispectral images and panchromatic images of SPOT6 and Landsat8 are fused, respectively, and the GS fusion method and the PC transformation method are compared. The fused image is shown in Figure 4. It can be seen from Figure 4 that the spatial resolution of the fused image has been improved. In contrast, the image after GS fusion is clearer and better maintains the texture features of the image.

For remote sensing images with different spatial resolutions, different construction land extraction methods have different applicability and their own advantages and disadvantages. In this study, SPOT6 and Landsat8 data are used to represent high-resolution images and medium-high-resolution images, respectively, to compare and improve construction land extraction methods. The extraction methods used include SVM method, neural network method, CART decision tree method, building index method, and rule-based object-oriented classification method.

Neural network method can establish complex relationship between input and output through self-learning. Therefore, the remote sensing images can be classified and processed effectively. Its advantage is that it has the ability to

Figure 4: Two data extraction methods for SPOT6 and Landsat8.

carry out strong nonlinear approximation and also has fault tolerance. The establishment of a decision tree is to classify and mine unknown data. SVM stands for support vector machine, which is a supervised learning model. It is commonly used for pattern recognition, classification, and regression analysis. The SVM algorithm supports linear classification and nonlinear classification and can also directly apply SVM to regression applications. At the same time, SVM can be applied in the field of multivariate classification by means of OVR or OVO. When using the CART decision tree method to extract construction land, this study uses the original multispectral images, NDVI (normalized difference vegetation index) calculation results, and ISODATA unsupervised classification results to construct a multivariate dataset. It uses the target object samples to automatically obtain expert knowledge rules. The building index method includes single index method and multi-index combination method, which is a commonly used method for rapid extraction of construction land. On the basis of image segmentation, the rule-based object-oriented classification method takes the image object with its own spatial characteristics as the basic processing unit, which alleviates the detailed information in the high-resolution image. It highlights the impact on the extraction of construction land and selects feature attributes to formulate rules for image information extraction. It is a method suitable for high spatial resolution remote sensing imagery.

5. Results and Discussion

5.1. Results

5.1.1. Area Change and Center of Gravity Shift. In this study, taking Tianjin Binhai New Area as an example, the remote sensing data of Landsat5 in 1996, 2001, 2006, and 2011 and Landsat8 in 2016 are selected for construction land extraction. Based on the comparison results of the extraction methods, the SVM method was selected to extract the construction land, and the construction land area of Tianjin Binhai New Area was obtained (Figure 5). From 1996 to 2016, the construction land area of Tianjin Binhai New Area increased from 183.88 km^2 to 294.86 km^2. The percentage of construction land in the total area of Binhai New Area increased from 9.27% in 1996 to 14.87% in 2016. The increased construction land area in the past 20 years is about 110.98 km^2, accounting for 60.36% of the construction land area in 1996.

From the calculation results of the expansion rate and expansion intensity of construction land, it can be seen in Figure 6(a) that from 1996 to 2016, the expansion rate and expansion intensity of construction land in Tianjin Binhai New Area showed an increasing trend, as shown in Figure 6(b). The year interval with the fastest expansion and the strongest expansion intensity is from 2011 to 2016. The area with the fastest expansion and the strongest expansion intensity is Tanggu District, followed by Hangu District.

From the contribution rate of construction land expansion in Tianjin Binhai New Area from 1996 to 2016 (Table 3), it can be seen that from 1996 to 2001, the expansion contribution rate of Tanggu District and Hangu District is not much different. After 2001, the contribution rate of construction land expansion in Tanggu District began to be significantly higher than the other two districts. After 2011, the expansion contribution of Dagang District began to grow significantly.

Figure 7 shows the migration trajectory of the overall center of gravity of Tanggu District, Hangu District, Dagang District, and Binhai New District. From 1996 to 2016, the center of gravity of construction land in Tanggu District shifted to the northeast as a whole, Hangu District shifted to the southwest, and Dagang District shifted to the northwest. Geographically, Hangu District is located in the northeast of Tanggu, and Dagang District is located in the southwest of Tanggu District. Therefore, the center of gravity of construction land in the three districts is gradually shifting to the trend of gathering. The center of gravity of construction land

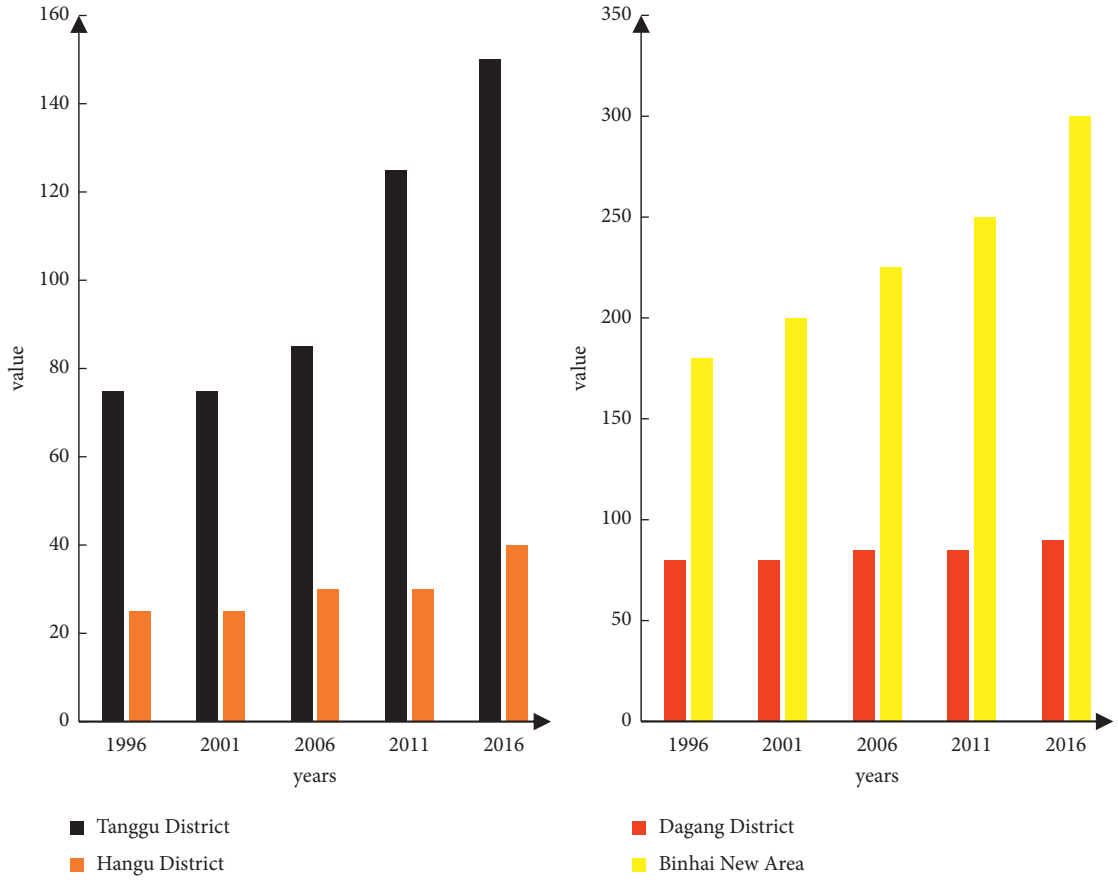

Figure 5: Changes in construction land in Tianjin Binhai New Area from 1996 to 2016.

in the entire Binhai New Area is regularly shifting to the north year by year.

5.1.2. Spatial Distribution and Morphological Changes. From the extraction results of construction land, the spatial distribution of construction land in Tianjin Binhai New Area in 1996, 2001, 2006, 2011, and 2016 is shown in Figure 8. It can be seen from Figure 9 that the construction land in Binhai New Area is concentrated in Tanggu District, Hangu District, and Dagang District, among which Tanggu District has the largest area. From 1996 to 2016, there were significant changes in construction land, and there is currently no significant increase in the concentration of construction land. It is just that there are different degrees of expansion in the original concentrated distribution area. Among them, the changes are most obvious in the Dagang urban area and the development zone.

It can be seen from Figure 8 that the number and density of construction land patches have become smaller. The average plaque area becomes larger, the degree of fragmentation decreases, and the proximity becomes higher. This shows that the construction land gradually changed from small patches with many to large patches with few. A similar small area of construction land is gradually expanded to form a larger area of construction land. The average proximity index and aggregation degree index gradually increased, indicating that the development trend of construction land from scattered distribution to aggregated distribution. The fractal dimension becomes larger, indicating that the shape of the construction land patch becomes more and more complex.

Fitting analysis is a statistical method used in finance and other fields to make predictions based on the observed values. In other words, it is a relative prediction that measures how the actual observed value is simulated. Through the fitting analysis, it is found that there is a strong nonlinear correlation between the construction land area and each shape index. The coefficient of determination R2 of NP, PD, MPS, MPI, AI, FD, and construction land area are 0.788, 0.850, 0.988, 0.956, 0.786, and 0.827, respectively. It can be seen that there is a strong correlation between construction land area and MPS. Because the construction land is not a natural feature, the change of the shape index of the construction land itself can reflect the influence of human factors on the shape and distribution of the construction land. Therefore, from a macroscopic point of view, the change of shape index also has certain regularity and correlation with the change of construction land.

5.2. Discussion. Construction land is the main material basis for residents to reside and live. Therefore, the population and human activities have a direct impact on the

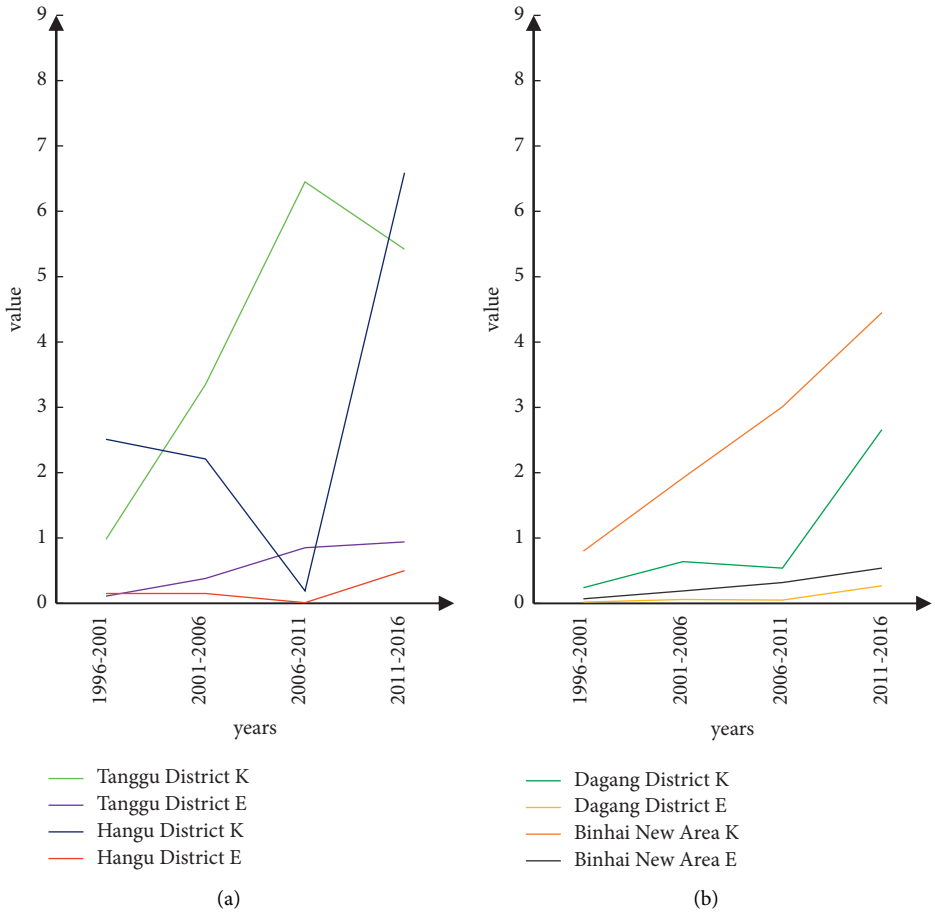

Figure 6: Expansion rate and expansion intensity of construction land in Binhai New Area from 1996 to 2016. (a) Expansion rate and expansion intensity of construction land in Binhai New Area. (b) Expansion rate and expansion intensity of Tanggu District and Hangu District.

scale and distribution of construction land. From 1996 to 2016, the registered population of Tianjin Binhai New Area increased by 26.49%, and the number of urban employees increased by 956,500. The rapid economic development has promoted the rapid increase of urban employees, and the nonagriculturalization of the agricultural population has become increasingly apparent. At the same time, the improvement of living standards and the requirements for housing and commercial places have also played a role in promoting the expansion of construction land. By fitting the area of construction land with the registered population and urban employees respectively in Figure 9, there is a more significant correlation between the area of construction land and the number of urban employees. It can be seen that population growth and the increase of urban employees are the main driving forces for the expansion of construction land.

5.2.1. Transportation Facilities. The development of transportation facilities has a driving effect on the expansion of construction land. Since the reform and opening up in Tianjin Binhai New Area, the construction of transportation facilities has been accelerated. In 1996, there were 828.67 kilometers of urban roads, 7,912,100 square meters, and 114 urban bridges. By 2011, Tianjin Avenue, Gangcheng Avenue, Jinbin Expressway, Beijing-Tianjin Expressway, Beijing-Tianjintang Expressway, and other express lanes were completed. The expressway network has taken initial shape, and a comprehensive transportation system with efficient, smooth, and distinct layers has been gradually formed. By 2016, a large number of new transportation facilities projects such as Tang-Han Expressway, Jin-Han Expressway, Jin-Han Link Line, and Jin-Gang Expressway have been completed. There are 140 bus lines and 2162 bus vehicles in the whole district. The annual passenger volume of public transport is about 130 million. A total of 642 rental vehicles were updated throughout the year, and 1,171 vehicles were operated by rental companies in the new district. The construction of transportation facilities and the development of transportation capacity not only promote the expansion process of construction land in Tianjin Binhai New Area, but also usually the construction land will expand along the main traffic roads within a certain range. Therefore, there is a certain relationship between the development and improvement of transportation facilities and the quantity and spatial distribution of construction land changes.

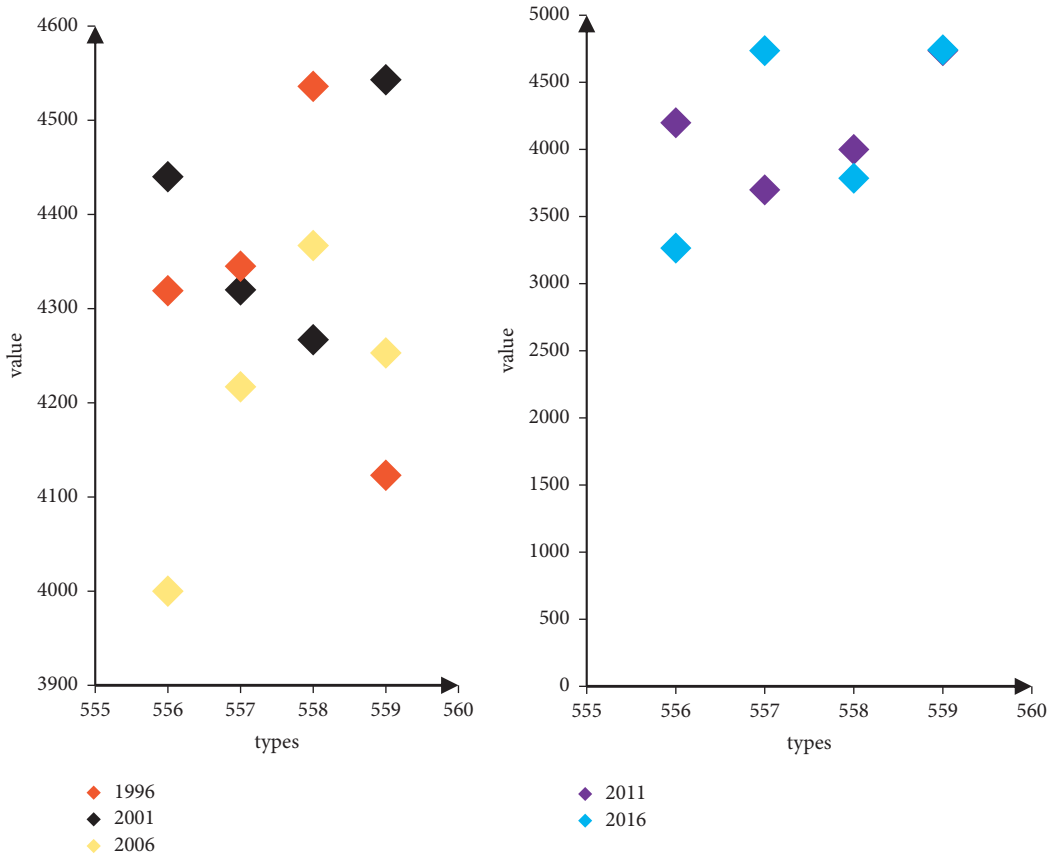

Figure 7: Coordinates of the center of gravity of construction land from 1996 to 2016.

5.2.2. Policy Orientation. National and regional macro land policies and urban planning have a significant impact on the expansion scale and expansion pattern of construction land. On the one hand, it guides the development direction of the city, and on the other hand, it has a certain role in regulating the scale and speed of urban development. From 1996 to 2016, the urban planning and construction of Binhai New Area achieved fruitful results. In March 1994, the development and construction of Binhai New Area kicked off. The overall planning concept in the initial stage of development and construction of Binhai New Area is to take Tianjin Port, development zone, and free trade zone as the skeleton and modern industry as the foundation to build a modern economic new zone with supporting infrastructure, complete service functions, and common development of finance, commerce, and tourism. It can be seen that Tianjin Port, development zone, and free trade zone are the key development areas of Tianjin Binhai New Area. Therefore, the launch of the Sino-Singapore Eco-city project is also one of the driving factors for the rapid change of construction land in Tianjin Binhai New Area after 2006. Therefore, it is inseparable from the support and regulation of policy factors whether the construction land has great changes in a short period of time. According to the spatial distribution of changes in construction land from 1996 to 2016, it can be seen that the changes in construction land in Tianjin Port, development zone, bonded zone, and nearby areas are more significant than other areas. These areas are mainly located in the northeastern part of Binhai New Area. Therefore, the center of gravity of construction land is also shifting to the northeast year by year. It can be seen that the main development areas of construction land are closely related to policy factors.

In summary, this study takes the comparison and improvement of construction land extraction methods as the main goal. It uses support vector machine method, neural network method, tram decision tree method, construction index method, and rule-based object-oriented classification method to extract construction land from SPOT6 and Landsat8 data. This section presents the basics of building datasets using high-resolution satellite imagery. The software and hardware components and construction steps of the building automatic extraction system are introduced. The realization of the main functions inside the automatic extraction system is introduced. The results of automatically extracting buildings are shown. The data evaluation index commonly used in the field of machine learning is used to analyze the accuracy of building extraction, and it is compared with other two neural network methods. On this basis, taking Tianjin Binhai New Area as an example, LandsatTM/OLI data is used. The SVM method was used to extract the construction land information for five years in 1996, 2001, 2006, 2011, and 2016.

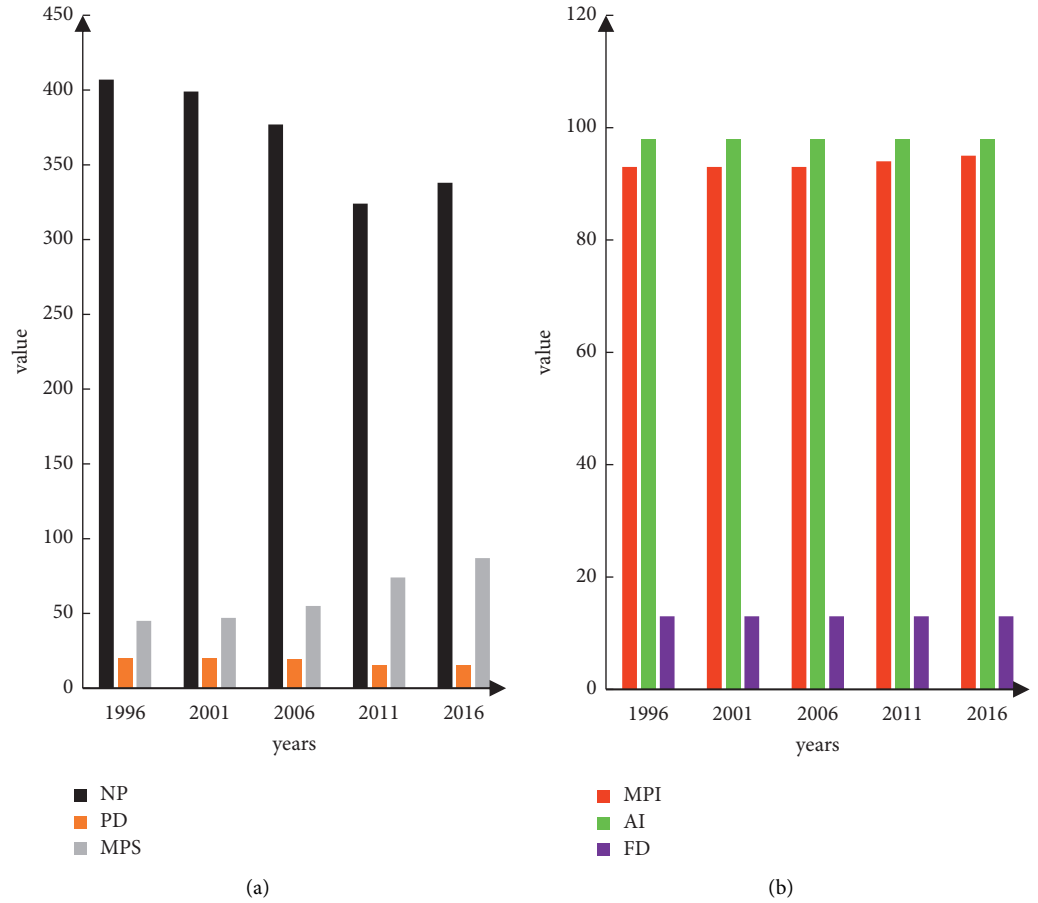

Figure 8: 1996–2016 Tianjin Binhai New Area Construction Land Shape Index. (a) NP, PD, and MPS values. (b) MPI, AI, and FD values.

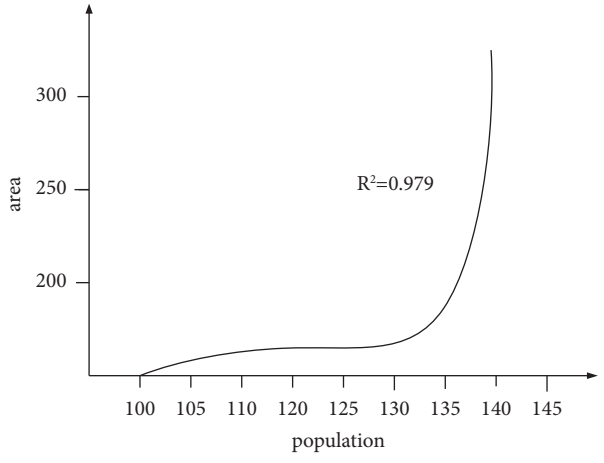

Figure 9: Fitting curve of construction land and population data.

6. Conclusions

The main conclusions of this study include the following points:

(1) It constructs construction land extraction rules for SPOT6 data and Landsat8 data respectively and proposes a construction land extraction index SBEI for SPOT6 data. Rule-based object-oriented methods can utilize the spatial and texture features of objects. To a certain extent, it can improve the influence of the phenomenon of homogeneity and heterogeneity on the extraction of ground objects. For SPOT6 images, the extraction accuracy of rule-based object-oriented method and SBEI index method is higher than that of SVM method, neural network method, and CART decision tree method. For Landsat8 images, SVM method and CART decision tree method have higher extraction accuracy.

(2) From 1996 to 2016, the area of construction land in Tianjin Binhai New Area continued to increase, and the expansion rate and expansion intensity increased. The largest contributor to expansion is Tanggu District. The center of gravity of construction land is gradually shifting to the northeast, and the center of gravity of construction land in Tanggu, Hangu, and Dagang is gradually converging. The patch density of construction land becomes smaller, and the average patch area becomes larger. In terms of spatial distribution, the degree of aggregation becomes higher and the morphology becomes more complex.

(3) The main factors affecting the change of construction land are population growth, economic development,

the construction of transportation facilities, and the drive of macro policies. Among them, the correlation between the construction land area and the urban employment population is higher than that of the registered population, and the correlation with the GDP of the secondary and tertiary industries is higher than that of the GDP of the primary industry.

Data Availability

No data were used to support this study.

Conflicts of Interest

The authors declare that they have no conflicts of interest.

Acknowledgments

The authors would like to thank my tutors and classmates for all their suggestions and assistance in writing this research.

References

[1] Q. Liu, "Retraction Note: application of remote sensing and GIS technology in urban ecological environment investigation," *Arabian Journal of Geosciences*, vol. 14, no. 24, pp. 2788–2791, 2021.

[2] N. Sofina and M. Ehlers, "Building change detection using high resolution remotely sensed data and GIS," *Ieee Journal of Selected Topics in Applied Earth Observations and Remote Sensing*, vol. 9, no. 8, pp. 3430–3438, 2016.

[3] B. K. Atak and E. E. Tonyalolu, "Evaluation of the effect of land use/land cover and vegetation cover change on land surface temperature: the case of Aydn province," *Turkish Journal of Forestry | Türkiye Ormancılık Dergisi*, vol. 21, no. 4, pp. 489–497, 2020.

[4] H. Dadashpoor and F. Salarian, "Urban sprawl on natural lands: analyzing and predicting the trend of land use changes and sprawl in Mazandaran city region, Iran," *Environment, Development and Sustainability*, vol. 22, no. 2, pp. 593–614, 2018.

[5] H. Ji and X. Luo, "Implementation of ensemble deep learning coupled with remote sensing for the quantitative analysis of changes in arable land use in a mining area," *Journal of the Indian Society of Remote Sensing*, vol. 49, no. 11, pp. 2875–2890, 2021.

[6] A. Frankl, J. Nyssen, E. Adgo, A. Wassie, and P. Scull, "Can woody vegetation in valley bottoms protect from gully erosion? Insights using remote sensing data (1938-2016) from subhumid NW Ethiopia," *Regional Environmental Change*, vol. 19, no. 7, pp. 2055–2068, 2019.

[7] R. Alshehhi, P. R. Marpu, W. L. Woon, and M. D. Mura, "Simultaneous extraction of roads and buildings in remote sensing imagery with convolutional neural networks," *ISPRS Journal of Photogrammetry and Remote Sensing*, vol. 130, no. aug, pp. 139–149, 2017.

[8] A. Mishra, K. Abdul Hakeem, V. V. Rao, P. V. N. Rao, and S. Chowdhury, "Assessment of colour changes in Lonar lake, Buldhana district, Maharashtra, India using remote sensing data," *Current Science*, vol. 120, no. 1, pp. 220–226, 2021.

[9] Z. Zheng, K. Fu, and C. Xu, "Remote sensing data user request merging technology," *Guofang Keji Daxue Xuebao/Journal of National University of Defense Technology*, vol. 41, no. 2, pp. 115–123, 2019.

[10] V. I. Lyalko, I. F. Romanciuc, L. A. Yelistratova, A. A. Apostolov, and V. M. Chekhniy, "Detection of changes in terrestrial ecosystems of Ukraine using remote sensing data," *Journal of Geology Geography and Geoecology*, vol. 29, no. 1, pp. 102–110, 2020.

[11] M. Yousif, "Hydrogeological inferences from remote sensing data and geoinformatic applications to assess the groundwater conditions: e," *Journal of African Earth Sciences*, vol. 152, no. APR, pp. 197–214, 2019.

[12] I. V. Eremenko, D. V. Dorofeeva, V. A. Romanyuk, and V. M. Pishchal'nik, "Research of changes in the ice cover of the Tatar strait based on data of remote sensing of the earth," *InterCarto InterGIS*, vol. 3, no. 23, pp. 20–31, 2017.

[13] S. M. Hassan and M. F. Sadek, "Geological mapping and spectral based classification of basement rocks using remote sensing data analysis: the Korbiai-Gerf nappe complex, South Eastern Desert, Egypt," *Journal of African Earth Sciences*, vol. 134, no. oct, pp. 404–418, 2017.

[14] N. Pazynych, "Valley complexes as ecosystem assets of heat island of urban agglomerations (on the example of the right-bank part of Kyiv)," *Ukrainian Journal of Remote Sensing*, vol. 3, no. 26, pp. 38–47, 2020.

[15] D. Dutta, K. Wang, E. Lee et al., "Characterizing vegetation canopy structure using airborne remote sensing data," *IEEE Transactions on Geoscience and Remote Sensing*, vol. 55, no. 2, pp. 1160–1178, 2017.

[16] F. Fakhri and I. Gkanatsios, "Integration of Sentinel-1 and Sentinel-2 data for change detection: a case study in a war conflict area of Mosul city," *Remote Sensing Applications Society and Environment*, vol. 22, no. 2, pp. 100505–100514, 2021.

[17] A. Iwan and K. K. Poon, "The role of governments and green building councils in cities' transformation to become sustainable: case studies of Hong Kong (east) and vancouver (west)," *International Journal of Sustainable Development and Planning*, vol. 13, no. 04, pp. 556–570, 2018.

[18] D. B. Alves and F. Perez-Cabello, "Multiple remote sensing data sources to assess spatio-temporal patterns of fire incidence over Campos Amazônicos Savanna Vegetation Enclave (Brazilian Amazon)," *Science of the Total Environment*, vol. 601-602, no. dec.1, pp. 601-602, 2017.

[19] R. Saboohi, H. Barani, M. Khodagholi, A. A. Sarvestani, and A. Tahmasebi, "Nomads' indigenous knowledge and their adaptation to climate changes in Semirom City in Central Iran," *Theoretical and Applied Climatology*, vol. 137, no. 1-2, pp. 1377–1384, 2019.

[20] S. Zoras, S. Veranoudis, and A. Dimoudi, "Micro- climate adaptation of whole building energy simulation in large complexes," *Energy and Buildings*, vol. 150, no. sep, pp. 81–89, 2017.

[21] K. Yao, A. Halike, L. Chen, and Q. Wei, "Spatiotemporal changes of eco-environmental quality based on remote sensing-based ecological index in the Hotan Oasis, Xinjiang," *Journal of Arid Land*, vol. 14, no. 3, pp. 262–283, 2022.

[22] A. Torabi Haghighi, H. Darabi, K. Shahedi, K. Solaimani, and B. Klove, "A scenario-based approach for assessing the hydrological impacts of land use and climate change in the marboreh watershed, Iran," *Environmental Modeling & Assessment*, vol. 25, no. 1, pp. 41–57, 2019.

[23] N. Nurda, R. Noguchi, and T. Ahamed, "Forest productivity and carbon stock analysis from vegetation phenological

indices using satellite remote sensing in Indonesia," *Asia-Pacific Journal of Regional Science*, vol. 4, no. 3, pp. 657–690, 2020.

[24] A. A. Lamqadem, H. Saber, and B. Pradhan, "Long-term monitoring of transformation from pastoral to agricultural land use using time-series landsat data in the feija basin (southeast Morocco)," *Earth Systems and Environment*, vol. 3, no. 3, pp. 525–538, 2019.

[25] S. S. Somvanshi, O. Bhalla, P. Kunwar, M. Singh, and P Singh, "Monitoring spatial LULC changes and its growth prediction based on statistical models and earth observation datasets of Gautam Budh Nagar, Uttar Pradesh, India," *Environment, Development and Sustainability*, vol. 22, no. 2, pp. 1073–1091, 2018.